Journal of Magnetism and Magnetic Materials 365 (2014) 51–55

Contents lists available at ScienceDirect

Journal of Magnetism and Magnetic Materials

journal homepage: www.elsevier.com/locate/jmmm

Critical end point of the first-order ferromagnetic transition in a $Sm_{0.55}(Sr_{0.5}Ca_{0.5})_{0.45}MnO_3$ single crystal

D. Mohan Radheep [a], P. Sarkar [b], S. Arumugam [a], R. Suryanarayanan [c], P. Mandal [d,*]

[a] Centre for High Pressure Research, School of Physics, Bharathidasan University, Tiruchirappalli 620 024, India
[b] Department of Physics, Serampore College, Serampore 712 201, India
[c] Laboratoire de Physico-Chimie de l'Etat Solide, ICMMO, CNRS, UMR8182, Universite Paris-Sud, 91405 Orsay, France
[d] Saha Institute of Nuclear Physics, 1/AF Bidhannagar, Calcutta 700 064, India

ARTICLE INFO

Article history:
Received 14 February 2014
Received in revised form
26 March 2014
Available online 28 April 2014

Keywords:
Perovskite manganite
First-order transition
Pressure effect

ABSTRACT

We report on the magnetic field (H) and hydrostatic pressure (P) dependence of the order of the ferromagnetic (FM) to paramagnetic phase transition in a $Sm_{0.55}(Sr_{0.5}Ca_{0.5})_{0.45}MnO_3$ single crystal. At ambient condition, the system exhibits a first-order FM transition at $T_C \approx 82$ K (in heating cycle) with strong thermal hysteresis (~ 13 K). The application of external H and P increases T_C, suppresses the hysteresis width, and thus weakens the first-order nature of the transition. Our analysis reveals that the hysteresis vanishes and the first-order FM transition becomes a crossover above a critical magnetic field $H_{cr} \approx 11.5$ T. The value of H_{cr} is highest among the manganite family, although the first-order nature of the FM transition is believed to be strongest in $Eu_{1-x}Sr_xMnO_3$ ($x \approx 0.45$).

1. Introduction

Perovskite manganites $RE_{1-x}AE_xMnO_3$ (RE: rare-earth ions, AE: alkaline-earth ions) have attracted much research interest, because of their several fascinating phenomena such as colossal magnetoresistance, electroresistance, piezoresistance, large magnetocaloric effect, charge–orbital ordering, phase separation, metal–insulator transition (MIT), and first-order ferromagnetic (FM) to paramagnetic (PM) phase transition [1–12]. For mixed valance manganites, the nature of the phase is mainly determined by the transfer interaction of e_g conduction electron between the neighboring Mn sites, i.e., the effective one-electron band-width, which can be tuned by a crystal lattice distortion in terms of the average A-site cation radius, $\langle r_A \rangle = \sum_i x_i r_i$, where x_i and r_i are respectively the fractional occupancies and effective ionic radii of A-site cations. Other than band-width, the size mismatch between RE and AE cations, generally termed as quenched disorder (QD), also plays an important role in determining the properties of manganites. The magnitude of QD can be evaluated by the A-site cation size variance, which is given by $\sigma^2 = \langle r_A^2 \rangle - \langle r_A \rangle^2 = \sum_i x_i r_i^2 - (\sum_i x_i r_i)^2$ [13]. From the electronic phase diagram of various $RE_{1-x}AE_xMnO_3$ crystals in the plane of $\langle r_A \rangle$ and σ^2, it is clear that the system with RE=Sm and AE=Sr can be considered as a narrowband manganite with relatively large QD [7]. The phase diagram of $Sm_{1-x}Sr_xMnO_3$ ($0.3 < x < 0.6$) shows that the system has a multicritical point close to half doping, where three phases FM metal ($x \leq 0.48$), charge–orbital ordered insulator ($x=0.49$ and 0.5), and A-type antiferromagnetic non-metal ($x \geq 0.51$) compete with each other [14,15]. Such a system, which is in the vicinity of a critical point may change its physical properties enormously even under a weak perturbation. Several studies on $Sm_{1-x}Sr_xMnO_3$ ($x = 0.45$–0.48) have shown that FM metal to PM insulator transition in this system is first-order in nature. The application of both external [such as magnetic field (H) and uniaxial/hydrostatic pressure (P)] and internal [such as A-site/B-site substitution or oxygen isotope exchange] perturbations affects the transition significantly [15–28]. The bandwidth and hence the ferromagnetic interaction in $Sm_{1-x}Sr_xMnO_3$ can be reduced further by the partial substitution of smaller cation Ca^{2+} in place of Sr^{2+} and, as a result, the competitive interactions, such as electron–lattice coupling, antiferromagnetic interaction between t_{2g} spins, and charge/orbital ordering, become comparable with FM double exchange interaction and the subtle balance between these interactions can result in unusual magnetoelectronic behaviors.

In this paper, we present the nature of FM to PM phase transition in $Sm_{1-x}(Sr_{1-y}Ca_y)_xMnO_3$ ($x=0.45$ and $y=0.5$) both at ambient condition as well as in the presence of external H and P. From the magnetic phase diagram of $Sm_{0.55}(Sr_{1-y}Ca_y)_{0.45}MnO_3$ ($0 \leq y \leq 1$), it is clear that with increasing y, FM transition temperature (T_C) decreases almost linearly up to $y \approx 0.6$ and just above that the system becomes charge ordered insulator [7]. So the present system, $Sm_{0.55}(Sr_{0.5}Ca_{0.5})_{0.45}MnO_3$ (SSCMO) lies in the border of two multicritical points: one is with respect to x and another is with respect to y and hence SSCMO is expected to be highly

* Corresponding author.
E-mail address: prabhat.mandal@saha.ac.in (P. Mandal).

http://dx.doi.org/10.1016/j.jmmm.2014.04.042
0304-8853/

susceptible to perturbations. Indeed, our analysis reveals that FM transition in SSCMO is strongly first-order and the application of external H and P increases the T_C and suppresses the first order nature of the transition. The value of the critical magnetic field (H_{cr}) at which the first-order FM transition becomes a crossover is ~11.5 T, which is highest among the manganite family.

2. Experimental details

Single crystals of $Sm_{0.55}(Sr_{0.5}Ca_{0.5})_{0.45}MnO_3$ were grown by the floating zone technique under oxygen atmosphere [29]. Phase purity was checked by the powder X-ray diffraction (XRD) method with Cu Kα radiation in a high resolution Rigaku TTRAX II diffractometer. We have not observed any impurity phase within the resolution (~2%) of XRD. All the peaks in the diffraction pattern were fitted well to an orthorhombic structure with *Pbnm* space group using the Rietveld method with an acceptance factor R_{Bragg} (%) = 1.33 and global χ^2 = 3.32 (Fig. 1). The lattice parameters obtained from the Rietveld refinements are a = 5.4085 Å, b = 5.4061 Å, and c = 7.6179 Å. The orientation of the crystal was determined from the position of the spots in the Laue pattern [Fig. 2] by indexing them using the Greninger chart. The crystal was also checked by a scanning electron microscope and an optical polarizing microscope, which reveal high quality surface of the crystal with a single domain. The crystal final composition determined by energy dispersive x-ray analysis is found to be close to the nominal composition. Another important measurement of crystal perfection in manganites is the ratio of the peak resistivity to the residual resistivity at low temperature, which is quite large ($\sim 3 \times 10^6$) in the studied crystal. The electrical resistivity was measured by a standard four-probe technique. The magnetization measurements at ambient condition and in the presence of hydrostatic pressure were performed by using the vibrating sample magnetometer module of a physical properties measurement system (Quantum Design) in fields up to 9 T. Magnetic field was applied only along the longest direction of the sample which is the (111) crystallographic direction. A clamp type miniature hydrostatic pressure cell (M Cell of Easylab, UK) made of non-magnetic Cu–Be alloy was used for the high-pressure magnetization measurements. A mixture of flourinert 70 and flourinert 77 was used as a pressure transmitting medium. The value of hydrostatic pressure was estimated from the shift of the superconducting critical temperature of pure Sn with applied pressure.

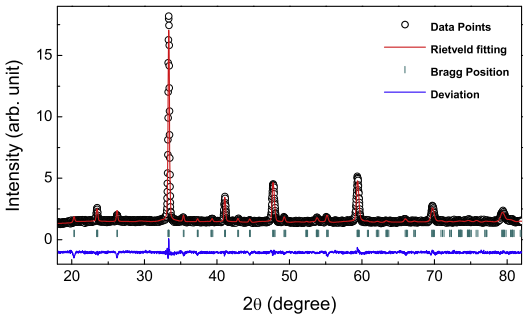

Fig. 1. X-ray diffraction pattern of $Sm_{0.55}(Sr_{0.5}Ca_{0.5})_{0.45}MnO_3$ (SSCMO) at room temperature. The red line corresponds to the Rietveld refinement of the diffraction pattern with space group *Pbnm*. (For interpretation of the references to color in this figure caption, the reader is referred to the web version of this paper.)

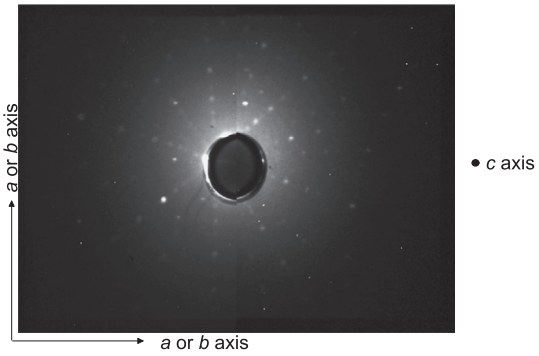

Fig. 2. Laue back reflection image of *c*-axis of the SSCMO single crystal.

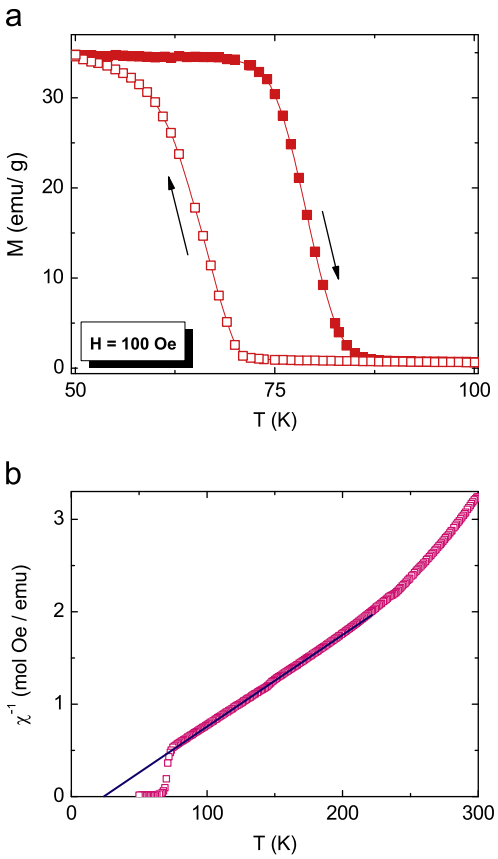

Fig. 3. Temperature dependence of (a) magnetization (M) and (b) inverse dc susceptibility ($\chi^{-1} = H/M$) for the SSCMO crystal at H = 100 Oe.

3. Experimental results

Fig. 3(a) shows the temperature dependence of dc magnetization (M) of SSCMO single crystal at H = 100 Oe. M shows a sharp change at T_C along with thermal hysteresis. The presence of hysteresis in $M(T)$ means that the system possesses two ambient T_C, whose values are ~82 K and ~69 K for heating and cooling cycles, respectively. The inverse dc susceptibility ($\chi^{-1} = H/M$) curve obtained from T dependence of M is displayed in Fig. 3(b). Above T_C, the departure of $\chi^{-1}(T)$ from the Curie–Weiss law [$\chi^{-1} = (T - \Theta)/C$, where Θ and C are the Weiss constant and Curie constant, respectively] indicates that the PM phase of this system is magnetically heterogeneous. From the slope of the approximate linear region of χ^{-1} vs T curve, we have calculated the value of C (~109 emu K mol^{-1} Oe^{-1}), and Θ (~24 K) is obtained from the linear extrapolation of $\chi^{-1}(T)$ to the temperature axis as shown in Fig. 3(b). The effective Bohr magneton number, P_{eff}, is evaluated from $C = (\mu_B P_{eff})^2 n/3k_B$, where n is the number of paramagnetic entities per mol. The value of P_{eff} is ~29.5, which is much larger

than that expected from the Curie–Weiss law for free Mn moments (P_{eff}=4.47), suggesting the presence of FM clusters composed of a few Mn^{3+} and Mn^{4+} ions.

Besides magnetization, we have also investigated the temperature dependence of resistivity (ρ) of the SSCMO crystal [Fig. 4(a)]. With increasing temperature, ρ increases very slowly until the MIT temperature (T_{MI}) is reached. At T_{MI}, ρ jumps abruptly as much as six orders of magnitude and then it shows activated semiconductor like behavior up to a fairly high temperature. The MIT in this system is extremely sharp and strongly hysteretic with temperature. Comparing $M(T)$ and $\rho(T)$ curves, one can see that T_C and T_{MI} are close to each other. The width of the resistivity transition can be characterized by the temperature coefficient of resistivity (TCR), which is defined as

$$TCR = \frac{1}{\rho}\left(\frac{d\rho}{dT}\right) \times 100\%. \quad (1)$$

As expected for a first-order transition, TCR exhibits a sharp peak close to T_{MI} [Fig. 4(b)]. The value of TCR and the transition temperature are important for the bolometric applications [30,31]. Several authors have performed this study on manganite thin films as well as bulk samples [30–32], and a quite large TCR (~23%/K) has been found in Ag-implanted La–Ca–Mn–O thin film [31]. From Fig. 4(b), one can see that the maximum TCR of SSCMO at T_{MI} is ~12%/K. Though this value is smaller than that observed in La–Ca–Mn–O thin films, it is relatively higher than those reported for several bolometric materials such as vanadium oxide, in which TCR is less than 5%/K [32].

Fig. 5(a) shows the temperature dependence of magnetization of SSCMO for different magnetic fields. With increasing H, the transition is shifted to higher temperatures at an average rate (dT_C/dH) of 7.15 K/T. The increase of T_C with H is a characteristic of colossal magnetoresistive manganites, especially in the presence

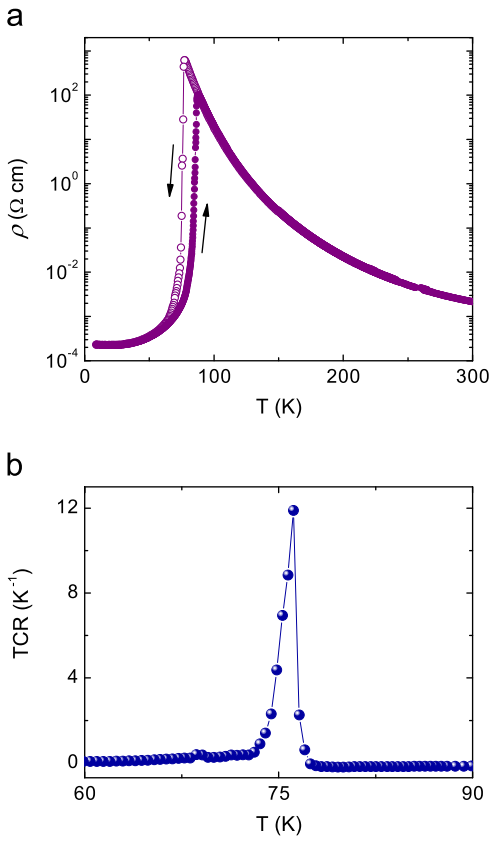

Fig. 4. Temperature dependence of (a) resistivity (ρ) and (b) temperature coefficient of resistance (TCR) for SSCMO.

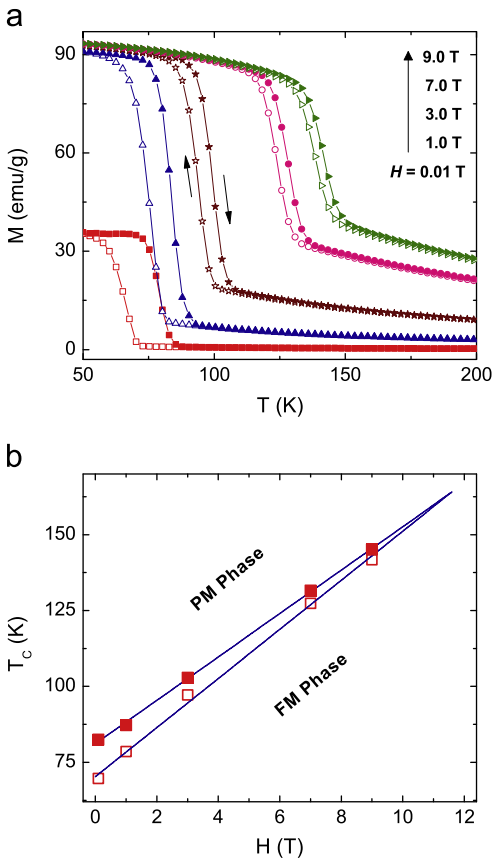

Fig. 5. (a) $M(T)$ curves of SSCMO for different magnetic fields. (b) $H-T$ phase diagram. Closed and open symbols are the transition temperatures derived from the heating and cooling cycles of $M(T)$ curves, respectively.

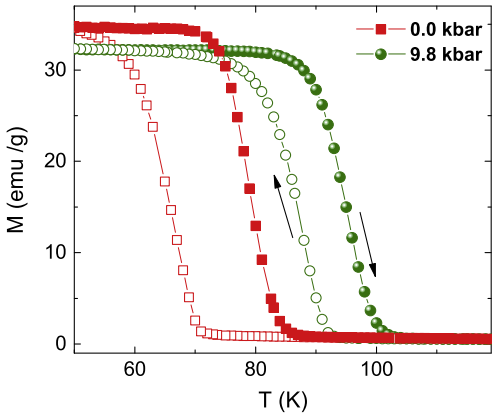

Fig. 6. Temperature dependence of magnetization in the presence of hydrostatic pressure at H=100 Oe.

of QD. The width of the thermal hysteresis in M gradually decreases with H and the two phase transition lines, corresponding to the heating and cooling cycles would merge to one another at a critical field, $H_{cr} \approx 11.5$ T and the corresponding critical temperature (T_{cr}) is ~164 K [Fig. 5(b)]. In the region between warming and cooling cycles, the magnetic state of the system is determined by the way through which the sample arrives at this region, i.e., by the increase or decrease of temperature. This confirms that SSCMO has a critical end-point ($H_{cr} \approx 11.5$ T, $T_{cr} \approx 164$ K) at which the first-order FM transition becomes a crossover. We have also investigated the effect of hydrostatic pressure on the nature of FM transition of SSCMO. Fig. 6 shows the representative plots of $M(T)$ curves at two different pressures

(0 and 9.8 kbar). Similar to H, external pressure extends the FM phase to higher temperature at the rate of ~17 K/GPa and reduces the thermal hysteresis [Fig. 6].

4. Discussions

The SSCMO crystal exhibits a strong first-order FM metal to PM insulator transition at $T_C \approx 82$ K. In the presence of both external H and P, T_C increases and the first order character of the FM transition is suppressed and eventually vanishes above a critical point. We would like to compare and contrast the present result on SSCMO with $Sm_{0.55}Sr_{0.45}MnO_3$ (SSMO). In the case of SSMO, resistivity changes by three orders of magnitude at MIT ($T_{MI} \sim 135$ K) along with thermal hysteresis of width 1.7 K [23]. So it is clear that in SSCMO, the change in resistivity at T_{MI} and the width of the hysteresis are respectively 2 orders of magnitude larger and 8 times wider as compared with SSMO, indicating that the first-order FM transition in SSCMO is much stronger than that for SSMO. The occurrence of first-order phase transition can be explained on the basis of strong coupling between magnetic and structural order parameters, i.e., between magnetization and average lattice distortion (Δ). The free energy (f) in the presence of coupling between M and Δ can be expressed as [33,34]

$$f = f_0 + AM^2 + BM^4 + CM^6 + \cdots + K\Delta^2 + \xi M^2\Delta, \quad (2)$$

where ξ represents the coupling between M and Δ. Taking the volume distortion that minimizes the free energy,

$$\frac{\partial f}{\partial \Delta} = 2K\Delta + \xi M^2 = 0, \quad (3)$$

$$\Delta = -\frac{\xi M^2}{2K}, \quad (4)$$

and inserting the value of Δ in Eq. (2), we obtain

$$f = f_0 + AM^2 + B_1M^4 + CM^6 + \cdots, \quad (5)$$

where $B_1 = (B - \xi^2/4K)$. If B_1 is positive, the sixth order term can be neglected in the vicinity of second-order transition. On the other hand, if B_1 is negative, the sixth order term is required to maintain the stability. In this case, as temperature is lowered, secondary minima develop and symmetrically placed about $M=0$. When the free energies of secondary minima with $M \neq 0$ pass through zero, there is a first-order transition [33]. If the coupling between magnetization and lattice distortion is very strong, i.e., ξ is large [$> \sqrt{(4KB)}$], B_1 becomes negative and leads the transition towards first-order. For manganites, the lattice distortion Δ is mainly determined by $\langle r_A \rangle^{-1}$. The value of $\langle r_A \rangle$ for SSMO is 1.21 Å. With the substitution of Ca, $\langle r_A \rangle$ starts to decrease and becomes 1.18 Å for SSCMO. This indicates that Δ and hence ξ is larger in SSCMO as compared to SSMO. So the coefficient B_1 should be more negative in SSCMO, suggesting that the first-order FM transition in SSCMO is stronger than in SSMO. Several studies have shown the strong dependence of structural properties on external H and magnetic properties on pressure or oxygen isotope substitution, suggesting that the magnetic and structural order parameters are coupled to each other [16,35]. To explain the reduction of T_C with Ca substitution, one has to consider the effect of both $\langle r_A \rangle$ and σ^2. T_C decreases with the decrease of $\langle r_A \rangle$ while increases with the decrease of σ^2 [13]. Similar to $\langle r_A \rangle$, σ^2 also decreases with Ca doping in SSMO. As the effect of $\langle r_A \rangle$ is stronger than the effect of σ^2 on T_C, T_C in SSCMO reduces with Ca doping. The above picture is also consistent with the polaronic model. As $\langle r_A \rangle$ reduces, charge carriers are more probable to be trapped by the lattice distortion and give rise to the formation of polarons–charge carriers accompanied by a localized distortion of the surrounding crystal lattice [4,36]. The polaron formation is primarily reflected through the activated like behavior of ρ [$\rho \sim \exp(E_g/kT)$, where E_g is the activation energy] above T_C. Both SSMO and SSCMO exhibit activated behavior of ρ with $E_g \sim 102$ meV and ~119 meV, respectively [23,24]. The deviation of $\chi^{-1}(T)$ from the Curie–Weiss behavior above T_C [Fig. 3(b)] is also an indication of the presence of polarons. The formation of polarons truncates the FM phase, enhances the self-trapping and drives the material towards a first-order phase transition.

The application of external perturbations weaken the coupling between magnetization and lattice distortion and, as a result, B_1 (Eq. (5)) starts to increase and becomes positive above a critical point where the first-order FM transition becomes a crossover or second-order [16,34,35]. It may be mentioned that the value of H_{cr} for SSMO is quite small (~3.75 T) and with the substitution of Nd (z) at Sm site [$(Sm_{1-z}Nd_z)_{0.55}Sr_{0.45}MnO_3$], T_C enhances and both H_{cr} and the width of thermal hysteresis decrease and eventually become zero at $z \approx 0.33$ [23,24]. Demkó et al. argued that the first-order nature of the FM transition is strongest in $Eu_{0.55}Sr_{0.45}MnO_3$ (ESMO) because ESMO has lowest $T_C \approx 50$ K and maximum thermal hysteresis width (14.3 K) among the manganites [23]. Furthermore, the resistivity jump across the transition is as high as ~9 orders of magnitude. So they claimed that the observed value of $H_{cr} \sim 7.4$ T for ESMO is the highest critical magnetic field in manganites. The present study, however, reveals that the value of H_{cr} in SSCMO is 1.5 times larger as compared to ESMO.

5. Conclusions

We have studied the effect of magnetic field and hydrostatic pressure on the nature of FM to PM phase transition in a single crystal of $Sm_{0.55}(Sr_{0.5}Ca_{0.5})_{0.45}MnO_3$. The strong hysteretic behavior of M and ρ with temperature and the abrupt decrease of ρ by several orders just below T_C suggest that the FM transition is discontinuous first-order in nature. External H and P increase the T_C and weaken the first-order character of the transition. We have identified a critical end point of the first-order FM transition and is given by ($H_{cr} \approx 11.5$ T, $T_{cr} \approx 164$ K). The observed value of H_{cr} is highest among the manganites.

Acknowledgments

The authors would like to thank Mr. A. Pal for technical assistance. S. Arumugam and D. Mohan Radheep acknowledge the financial supports from DST (SERB and TSDP), UGC and CSIR-SRF, New Delhi.

References

[1] Y. Tokura, Rep. Prog. Phys. 69 (2006) 797.
[2] C.N.R. Rao, B. Raveau, Colossal Magnetoresistance, Charge Ordering and Related Properties of Manganese Oxides, World Scientific, Singapore, 1998.
[3] E. Dagotto, T. Hotta, A. Moreo, Phys. Rep. 344 (2001) 1.
[4] M.B. Salamon, M. Jaime, Rev. Mod. Phys. 73 (2001) 583.
[5] P.K. Siwach, H.K. Singh, O.N. Srivastava, J. Phys.: Condens. Matter 20 (2008) 273201.
[6] Y. Tokura, H. Kuwahara, Y. Moritomo, Y. Tomioka, A. Asamitsu, Phys. Rev. Lett. 76 (1996) 3184.
[7] Y. Tomioka, Y. Tokura, Phys. Rev. B 70 (2004) 014432.
[8] R. Mohan, N. Kumar, B. Singh, N.K. Gaur, S. Bhattacharya, S. Rayaprol, A. Dogra, S.K. Gupta, S.J. Kim, R.K. Singh, J. Alloys Compd. 508 (2010) L32;
S.T. Mahmud, M.M. Saber, H.S. Alagoz, K. Biggart, R. Bouveyron, Mahmud Khan, J. Jung, K.H. Chow, Appl. Phys. Lett. 100 (2012) 232406.
[9] H.Y. Hwang, T.T.M. Palstra, S-W. Cheong, B. Batlogg, Phys. Rev. B 52 (1995) 15046;
V. Laukhin, J. Fontcuberta, J.L. Garcia-Munoz, X. Obradors, Phys. Rev. B 56 (1997) R10009.

[10] I.V. Medvedeva, Y.S. Bersenev, K. Bärner, L. Haupt, P. Mandal, A. Poddar, Physica B 229 (1997) 194.
[11] S. Arumugam, K. Mydeen, N. Manivannan, M.K. Vanji, D. Prabhakaran, A.T. Boothroyd, R.K. Sharma, P. Mandal, Phys. Rev. B 73 (2006) 212412;
R. Thiyagarajan, N. Manivannan, S. Arumugam, S.E. Muthu, N.R. Tamilselvan, C. Sekar, H. Yoshino, K. Murata, M.O. Apostu, R. Suryanarayanan, A. Revcolevschi, J. Phys.: Condens. Matter 24 (2012) 136002.
[12] M.H. Phan, S.C. Yu, J. Magn. Magn. Mater. 308 (2007) 325, and references herein.
[13] L.M. Rodriguez-Martinez, J.P. Attfield, Phys. Rev. B 54 (1996) R15622;
L.M. Rodriguez-Martinez, J.P. Attfield, Phys. Rev. B 63 (2000) 024424.
[14] C. Martin, A. Maignan, M. Hervieu, B. Raveau, Phys. Rev. B 60 (1999) 12191.
[15] Y. Tomioka, H. Hiraka, Y. Endoh, Y. Tokura, Phys. Rev. B 74 (2006) 104420.
[16] H. Kuwahara, Y. Moritomo, Y. Tomioka, A. Asamitsu, M. Kasai, R. Kumai, Y. Tokura, Phys. Rev. B 56 (1997) 9386;
Y. Tomioka, H. Kuwahara, A. Asamitsu, M. Kasai, Y. Tokura, Appl. Phys. Lett. 70 (1997) 3609.
[17] N.A. Babushkina, E.A. Chistotina, O.Yu. Gorbenko, A.R. Kaul, D.I. Khomski, K.I. Kugel, Phys. Rev. B 67 (2003) 100410 (R);
G.S. Chang, E.Z. Kurmaev, L.D. Finkelstein, N.A. Babushkina, A. Moewes, T.A. Callcott, Phys. Rev. B 74 (2006) 125105.
[18] L.M. Fisher, A.V. Kalinov, I.F. Voloshin, N.A. Babushkina, D.I. Khomshkii, Y. Zhang, T.T.M. Palstra, Phys. Rev. B 70 (2004) 212411.
[19] P. Sarkar, P. Mandal, P. Choudhury, Appl. Phys. Lett. 92 (2008) 182506.
[20] P. Sarkar, P. Mandal, Appl. Phys. Lett. 92 (2008) 052501.
[21] P. Sarkar, P. Mandal, A.K. Bera, S.M. Yusuf, L.S.S. Chandra, V. Ganesan, Phys. Rev. B 78 (2008) 012415.
[22] K. Mydeen, P. Sarkar, P. Mandal, A. Murugeswari, C.Q. Jin, S. Arumugam, Appl. Phys. Lett. 92 (2008) 182510.
[23] L. Demkó, I. Kézsmárki, G. Mihály, N. Takeshita, Y. Tomioka, Y. Tokura, Phys. Rev. Lett. 101 (2008) 037206.
[24] P. Sarkar, P. Mandal, A.K. Bera, S.M. Yusuf, S. Arumugam, C.Q. Jin, T. Ishida, S. Noguchi, Phys. Rev. B 79 (2009) 144431.
[25] A. Murugeswari, P. Sarkar, S. Arumugam, N. Manivannan, P. Mandal, T. Ishida, S. Noguchi, Appl. Phys. Lett. 94 (2009) 252506.
[26] P. Sarkar, S. Arumugam, P. Mandal, A. Murugeswari, R. Thiyagarajan, S.E. Muthu, D.M. Radheep, C. Ganguli, K. Matsubayshi, Y. Uwatoko, Phys. Rev. Lett. 103 (2009) 057205.
[27] S. Arumugam, P. Sarkar, P. Mandal, A. Murugeswari, K. Matsubayashi, C. Ganguli, Y. Uwatoko, J. Appl. Phys. 107 (2010) 113904.
[28] D. Mohan Radheep, P. Sarkar, S. Arumugam, P. Mandal, Appl. Phys. Lett. 102 (2013) 092406.
[29] P. Mandal, B. Bandyopadhyay, B. Ghosh, Phys. Rev. B 64 (2001) 180405;
P. Mandal, B. Ghosh, Phys. Rev. B 68 (2003) 014422;
T. Chatterji, B. Ouladdiaf, P. Mandal, B. Ghosh, Solid State Commun. 131 (2004) 75.
[30] A. Goyal, M. Rajeswari, R. Shreekala, S.E. Lofland, S.M. Bhagat, T. Boettcher, C. Kwon, R. Ramesh, T. Venkatesan, Appl. Phys. Lett. 71 (1997) 2535;
R. Shreekala, M. Rajeswari, S.P. Pai, S.E. Lofland, V. Smolyaninova, K. Ghosh, S.B. Ogale, S.M. Bhagat, M.J. Downes, R.L. Greene, R. Ramesh, T. Venkatesan, Appl. Phys. Lett. 74 (1999) 2857.
[31] R. Bathe, K.P. Adhi, S.I. Patil, G. Marest, B. Hannoyer, S.B. Ogale, Appl. Phys. Lett. 76 (2000) 2104.
[32] Y. Sun, M.B. Salamon, S.H. Chun, J. Appl. Phys. 92 (2002) 3235.
[33] P.M. Chaikin, T.C. Lubensky, Principles of Condensed Matter Physics, Cambridge University Press, Cambridge, UK, 1995.
[34] M. Otero-Leal, F. Rivadulla, J. Rivas, Phys. Rev. B 76 (2007) 174413.
[35] A.N. Styka, Y. Ren, N.A. Babushkina, D.E. Brown, J. Appl. Phys. 100 (2006) 103520.
[36] R.M. Kusters, J. Singleton, D.A. Keen, R.M. Greevy, W. Hayes, Physica B 155 (1989) 362;
M.F. Hundley, M. Hawley, R.H. Heffner, Q.X. Jia, J.J. Neumeier, J. Tesmer, J.D. Thompson, X.D. Wu, Appl. Phys. Lett. 67 (1995) 860;
J.M. De Teresa, M.R. Ibarra, P.A. Algarabel, C. Ritter, C. Marquina, J. Blasco, J. Garcia, A. Del Moral, Z. Arnold, Nat. Lond. 386 (1997) 256.